JPL Publication 91-32

Upper Bound SEU Rate for Devices in an Isotropic or Nonisotropic Flux

Larry D. Edmonds

August 1, 1991

National Aeronautics and
Space Administration

Jet Propulsion Laboratory
California Institute of Technology
Pasadena, California

JPL Publication 91-32

Upper Bound SEU Rate for Devices in an Isotropic or Nonisotropic Flux

Larry D. Edmonds

August 1, 1991

National Aeronautics and
Space Administration

Jet Propulsion Laboratory
California Institute of Technology
Pasadena, California

The research described in this publication was carried out by the Jet Propulsion Laboratory, California Institute of Technology, under a contract with the National Aeronautics and Space Administration (NASA). It was sponsored by the NASA Microelectronics Radiation Effects Ground Test Program.

ABSTRACT

A method for constructing upper bound estimates for device single event upset (SEU) rates is proposed. A directional Heinrich flux, as a function of direction, must be known. A computer code, included in this publication, converts the directional Heinrich flux into an "effective flux". The effective flux provides a simple way to estimate upper bound SEU rates for devices with a known normal incident cross section versus LET curve.

CONTENTS

1. INTRODUCTION

Particle sources that can cause single event upset (SEU) in integrated circuits include solar events, the anomalous component (which is important in some low Earth orbits), and trapped heavy ions around a planet (e.g., Jupiter). For many space projects, one or another of these components will dominate the mission integrated fluence (which determines the probability of an SEU during the mission) and/or peak flux (which impacts the effectiveness of some error detection and correction schemes). Thus, for many space projects, one or another of the above components is the most important SEU related environment. All of these components are relatively soft in the sense that mass shielding can cause significant attenuation. Galactic cosmic rays are hard (only slightly attenuated by mass shielding) but are frequently not the environment that causes a space project the most trouble. The most trouble often comes from the softer components. Because these components are affected by mass shielding, and such shielding is rarely symmetrically distributed in a spacecraft, the flux inside a spacecraft is not isotropic. Therefore, there is a need for the ability to estimate SEU rates in a nonisotropic flux. A particular calculational method is presented here. The calculational method applies to SEU caused by direct ionization. Proton induced SEU involving nuclear reaction products requires a separate calculation which is not discussed here.

The SEU rate for a device can be expressed as

$$\text{rate} = \int_0^{\infty} \int_{-1}^{1} \int_0^{2\pi} h(L,\theta,\phi)\ \sigma(L,\theta,\phi)\ d\phi\ d(\cos\theta)\ dL \qquad (1)$$

where $h(L,\theta,\phi)$ is the differential (in LET) directional flux evaluated at LET L and at the spherical coordinate angles θ and ϕ (the Z axis is normal to the device). σ is a LET dependent directional cross section.

The best determination of σ typically comes from heavy ion tests using particle accelerators. (There are special conditions, discussed in section 4, where σ can be deduced from a simple physical model. The present discussion applies to the more common situation where σ is known only from heavy ion tests.) If σ was known in sufficient detail (it is assumed that the flux, h, is known), the rate could be evaluated by numerically evaluating the integral in (1). Unfortunately, σ is usually only partially determined from experimental data because data at large θ is not meaningful (i.e., does not apply to particles found in space) unless the test ions have a lot of range. Machines capable of producing such long range ions (e.g., the Bevalac) are expensive to use and, therefore, most SEU tests do not use such machines. JPL normally tests with lower energy machines and restricts θ to be between 0 and 60°. With θ so restricted, the "cosine law", which states that

$$\sigma(L,\theta,\phi) \approx |\cos\theta|\ \sigma(L/|\cos\theta|,0,0)\ , \qquad (2)$$

is usually observed. The large θ (large enough to violate (2)) behavior is usually not measured.

Because the large θ behavior of σ is usually unknown, it is necessary to make worst-case assumptions, i.e., we look for an upper bound for the SEU rate. This will be done by assuming a particular physical model and adjusting unknown parameters to obtain a maximum predicted rate[1] (details are discussed later).

---

1. Some devices exhibit a significant deviation from the cosine law for angles as small as 60° or less. For such devices, the existing data qualifies as large angle data (the tested angles are large enough to violate (2)) and it is possible to justify SEU rate estimates that are less pessimistic than the upper bound estimates considered here. Instead of adjusting model parameters for a maximum predicted rate, they are adjusted for a best fit to the measured data.

There are circumstances where upper bound estimates can overestimate the actual SEU rate by orders of magnitude. This can occur when h is of such a form that the SEU rate can be dominated by particles that hit the device at grazing angles ($\theta \approx 90°$). In this case, the most important angles are the large angles (beyond the range such that (2) applies), and typical experimental data is inadequate because the test is performed at the least important angles. There are no data pertaining to the most important angles, and the data leave SEU rates undetermined by orders of magnitude. An estimate that is an upper bound (i.e., large enough to compensate for the inadequacy of the data) could be orders of magnitude larger than the actual rate.

Upper bound estimates are occasionally (not always) much higher than the actual SEU rate, but such estimates can still be useful to a space project. It often happens that a device is hard and/or the environment is mild, so that even an excessively pessimistic prediction does not bother the project. If this is the case, an upper bound estimate is good enough. If not, the project might have to obtain and utilize large incident angle cross section data so a less pessimistic estimate can be obtained. This was done in the past by JPL, but the expense was considerable.

Because upper bound estimates are useful and more economical than accurate methods, they are the final objective of this publication. However, as a means to an end, the SEU rate will also be expressed as a function of the parameters of a particular physical model. This allows the rate to be estimated when the parameters happen to be known. Most of the analysis to follow is concerned with expressing the rate in terms of model parameters. Adjusting the parameters to maximize the rate is discussed in Sections 7 and 8. The "maximized rate" can be used to construct an "effective flux" which greatly simplifies SEU rate calculations (see Sections 7 and 8).

2. THE PHYSICAL MODEL

We will use the credible (but nonrigorous) assumption that there will be enough pessimism in our treatment of the θ dependence of σ to more than compensate for any possible ϕ dependence. In other words, we assume that an upper bound estimate, derived for devices with azimuthal symmetry, will over-estimate an actual SEU rate even if the actual device does not have azimuthal symmetry. Thus, we confine our attention to devices with azimuthal symmetry and $\sigma(L,\theta)$ will replace $\sigma(L,\theta,\phi)$.

Another assumption is that the device consists of a number of charge-collecting volumes and an SEU occurs when one of these volumes collects an amount of charge that exceeds some critical value. It is also assumed that the charge collected by a volume is proportional to ion path length (in the volume) times ion LET (this is a traditional assumption [1]). For the reasons given in the previous paragraph, we will confine our attention to circular-cylindrical charge-collecting volumes.

3. DISCUSSION OF SINGLE CHARGE-COLLECTING VOLUME

Devices containing a collection of charge-collecting volumes will eventually be considered, but the analysis will begin with a device (hypothetical or real) containing a single charge-collecting volume of uniform thickness. The normal incident cross section versus LET curve for such a device is a step function of height A and with a threshold LET L_{th}. The charge-collecting volume is assumed to be a circular cylinder of normal incident area A and a threshold LET L_{th} is associated with it. The only parameter that cannot be determined from the normal incident cross section data is the charge-collecting volume thickness T. An upper bound SEU rate estimate is obtained by maximizing the predicted rate in T with A and L_{th} held fixed.

It is interesting that the "cosine law" becomes exact (i.e., (2) becomes exact for all θ) in the limit as $T \to 0$ and many people erroneously think that this limit gives the maximum SEU rate. So-called "proofs" of this assertion are flawed because they fail to include particle trajectories that enter the volume through a side instead of the upper surface. In reality, a plot of rate versus T will show a maximum at some nonzero T. An extreme case that illustrates this occurs when L_{th} is so small compared to the LET of all particles in the environment that virtually every particle that hits the volume will cause an upset. In this case, the SEU rate will increase as T increases because more particles hit the volume when T is larger. Thus the upper bound SEU rate is not obtained from the limiting case as $T \to 0$[1].

Determination of the maximum (in T) rate requires that we be able to estimate the rate for arbitrary T. This is a nontrivial calculation and a simplifying approximation is helpful. For a given trajectory direction, we can place an imaginary box-shaped volume around the charge-collecting volume which is oriented relative to the trajectory direction as shown in Figure 1. Any trajectory that hits the charge-collecting volume will also hit the imaginary box, and have a path length in the box that is at least as large as that in the original volume. The path length required for an SEU is the same for the two volumes (both volumes are assigned the same normal incident threshold LET and have the same thickness) so any particle that causes SEU in the original volume will also do so in the imaginary box. Therefore, an upper bound for $\sigma(L,\theta)$ can be estimated by replacing the original volume with the imaginary box. The box is conveniently oriented so that the mathematical analysis (see Section 5) is essentially two dimensional. Note that the box has a different orientation for different values of the trajectory coordinate ϕ. For this

---

1.The limiting ($T \to 0$) rate often is very nearly equal to the maximum (in T) rate. But this condition, when it holds, is a property of h and L_{th} and does not apply to all possible h and L_{th} (as the above counter-example has shown).

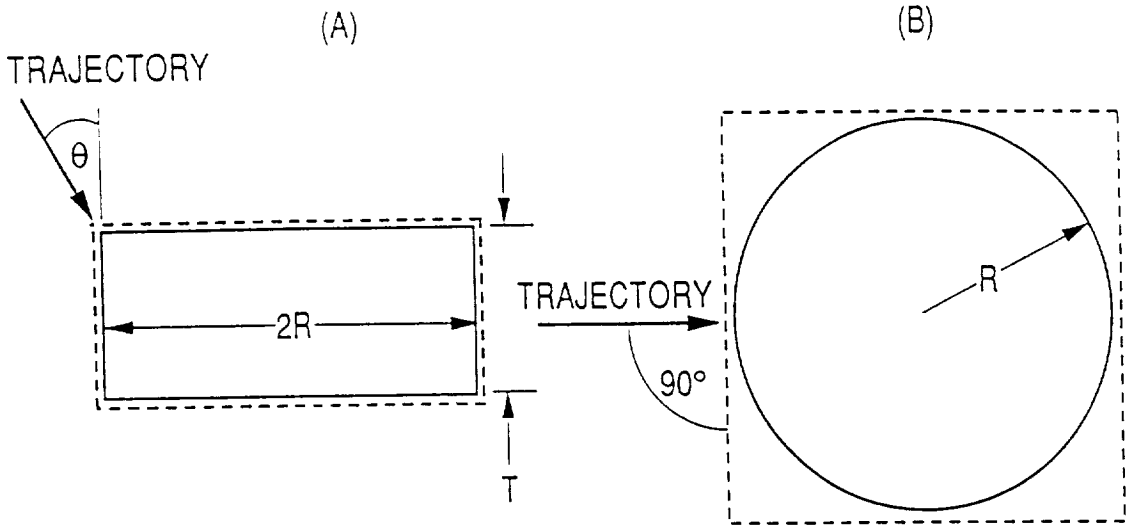

Figure 1. Two views of the charge-collecting volume (solid curves) and an imaginary box-shaped volume (dotted curves). (A) is a view from a side with the Z axis and particle trajectory in the plane of the paper. (B) is a view from above.

reason, the box will be called the "rotating box".

4. UTILIZATION OF DEVICE FEATURE GEOMETRY

Until now, it was assumed that the only available device data is that obtained from heavy ion tests. Occasionally, the geometry of various structures (e.g., depletion regions) is known. It is tempting to utilize such information, when it is available, and this section discusses when and how such information should be utilized. Throughout this discussion, it is assumed that the charge-collecting volume is a depletion region (DR).

If the DR thickness happens to be known, it is tempting to set T equal to this thickness (some people also add a "funnel length" but this is a mistake and is discussed again later). If this is valid, it is better than selecting T for a maximum rate because it will produce an accurate rate estimate instead of an upper bound estimate. However, it is often not valid to set T equal to the DR thickness, because the physical model (which assumes collected charge to be proportional to LET times path length in a geometrically well-defined volume) is totally wrong when diffusion plays a role.

It is nontrivial to determine when diffusion plays a role (even if device time constants are known) because diffusion is both fast and slow. If an ion track is close to a DR, there is initially a very large carrier gradient between the high density track and the sink-like DR boundary. This large gradient produces a very strong diffusion current (fast charge collection) which is comparable to the drift current during the recovery stage of funneling (virtually all charge collection occurs during the recovery stage of funneling [2]). As the track dissipates, charge collection via diffusion slows down, but a significant charge can be collected quickly. Simulations, using a cylindrical coordinate version of PISCES, have shown that an ion track can obliterate a

DR that is 5μm away in 0.3ns. Closer tracks can do the same in a shorter time.

Although the physical model is wrong when diffusion plays a role, an approximate cosine law (for a limited angle range) is compatible with diffusion and the physical model can be used in a curve fitting sense. When applied to diffusion, the charge-collecting volume dimensions that produce the correct SEU rate prediction are not the dimensions of any actual physical structures. Therefore, dimensions should be determined from heavy-ion cross section data, if large angle data are available, and not from device feature geometry. If large angle data are not available, the appropriate dimensions are unknown; hence the need for upper bound estimates.

If it is somehow known that diffusion can be neglected for a particular device, it should be acceptable to set T equal to the DR thickness. Many people erroneously think that a "funnel length" should be added to the DR thickness. A recent funneling analysis [2] concludes that, in the absence of diffusion, total collected charge from an ion track can be calculated from the physical model (which states that collected charge is proportional to path length times LET) by extending each DR linear dimension (including the lateral dimensions) by a certain percentage. The DR can be replaced with an "extended DR" for the purpose of calculating collected charge. This reinforces the concept of adding a "funnel length" to the dimensions, but the concept correctly calculates only charge collected from a given track intersecting the DR. The concept of an extended DR does not correctly calculate the cross section. Trajectories intersecting only the extended portions do not result in a collected charge (in the absence of diffusion). The funnel length extension of the DR does not contribute to the cross section. Hence an extended DR cannot play the role of the charge-collecting volume if our simple physical model is to be used.

It was concluded above that an extended DR should not be used to determine the charge-collecting volume dimensions. However, the actual DR (no funnel lengths added) can be used in the absence of diffusion. The reason is that the total collected charge is proportional to the charge liberated in the DR [2]. If total collected charge has a threshold or critical value which results in SEU, then so does the charge liberated in the actual DR. The latter charge can be calculated by applying the simple physical model to the actual DR (no funnel lengths are added).

In summary, if the importance of diffusion is unknown, it is best not to utilize geometric data because we could be putting the "right information into the wrong model". A charge-collecting volume is a mathematical construct whose dimensions should be determined from large angle heavy ion cross section data. In the absence of such data, the appropriate dimensions are unknown; hence the need for upper bound estimates. If it is known that diffusion can be neglected, the appropriate dimensions for the charge-collecting volume are the actual DR dimensions (funnel lengths are not added). Note that the threshold value of charge liberated in the DR, rather than the threshold value of collected charge, is used to determine the threshold LET (but this is irrelevant if threshold LET is known from heavy ion tests).

5. MATHEMATICAL ANALYSIS FOR SINGLE CHARGE-COLLECTING VOLUME[1]

The objective is to calculate the SEU rate, as a function of A (the normal incident area of the original volume), T, and L_{th} . R is the radius of the original volume and is related to A by $R=(A/\pi)^{1/2}$. An upper bound estimate will be obtained by replacing the original volume with the rotating box (of width 2R) discussed

---

1.Readers that are not interested in the mathematical details can skip this section.

in Section 3. Throughout this section, the cross section $\sigma(L,\theta)$ refers to the rotating box rather than the original volume.

We begin the analysis by assuming that θ satisfies $0<\theta<90°$, which represents particles moving in a downward direction. σ is expressed as the sum of four partial cross sections

$$\sigma(L,\theta) = \sigma_1(L,\theta) + \sigma_2(L,\theta) + \sigma_3(L,\theta) + \sigma_4(L,\theta)$$

where σ_i is the cross section associated with the i^{th} group of particle trajectories and the groups are defined by (for $\theta\epsilon(0,\pi/2)$):

group 1 = Trajectories that enter the box through the upper surface and exit through the lower surface.

group 2 = Trajectories that enter the box through the upper surface and exit through a side.

group 3 = Trajectories that enter the box through a side and exit through the lower surface.

group 4 = Trajectories that enter the box through a side and exit through a side.

The analysis is slightly different depending on whether $\theta\epsilon(0,\arctan(2R/T))$ or $\theta\epsilon(\arctan(2R/T),\pi/2)$ and the two cases are considered separately. Group 1 trajectories are illustrated for the first case in Figure 2. These trajectories all have the same path length, l (see Figure 2), and SEU will occur if l and particle LET, L, are related by

$$l\ L \geq L_{th}\ T$$

or

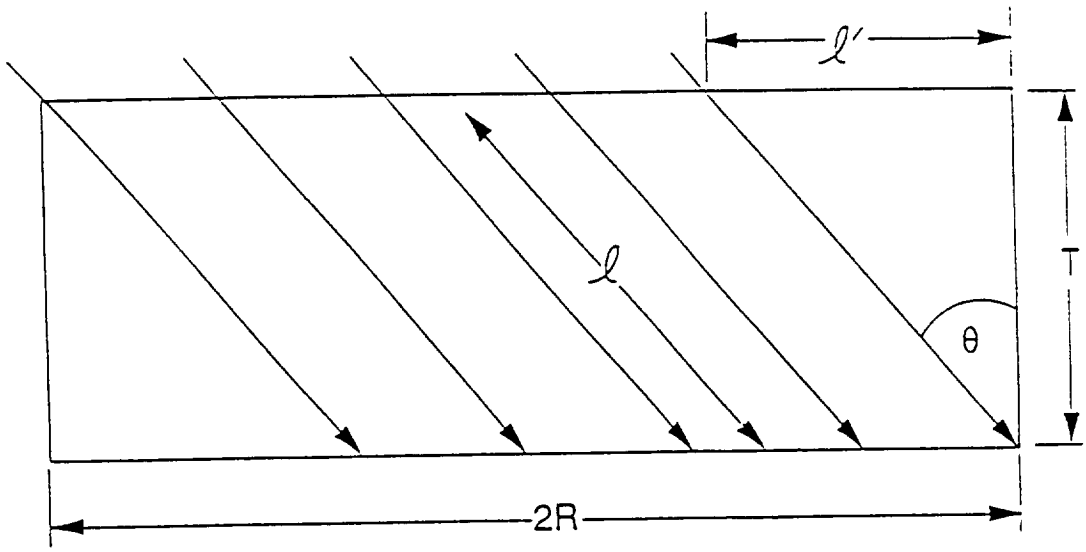

Figure 2. Illustration of group 1 trajectories when $0<\theta<\arctan(2R/T)$.

$$L \geq L_{th} \cos\theta \ . \qquad (3)$$

These trajectories can enter the box through any point in the upper surface (of area $4R^2$) except the section of width l' (and area 2Rl') shown in the figure. Hence, the trajectories can enter through any point of a surface of area

$$4R^2 - 2R\ l' = 2R\ (2R - T\ \tan\theta).$$

The cross section (when (3) is satisfied) is the projection of this area in the direction of the trajectory. This gives:

$$\text{If } 0 \leq \theta \leq \arctan(2R/T) \text{ then}$$

$$\sigma_1(L,\theta) = \begin{cases} 2R\ (2R - T\ \tan\theta)\ \cos\theta & \text{if } \cos\theta < L/L_{th} \\ 0 \quad \text{otherwise.} \end{cases}$$

If $\arctan(2R/T)<\theta<\pi/2$, there are no group 1 trajectories and we get:

$$\text{If } \arctan(2R/T) < \theta < \pi/2 \text{ then}$$
$$\sigma_1(L,\theta) = 0.$$

Figure 3 illustrates group 2 trajectories for the case $0<\theta<\arctan(2R/T)$. SEUs are caused by trajectories below the one with length, l (see Figure 3), satisfying

$$l = L_{th}\ T/L \qquad (4)$$

and such trajectories intersect a surface section of height l' (and area 2Rl') shown in the figure, where

$$l' = T - l\ \cos\theta = T - (L_{th}\ T/L)\ \cos\theta \ .$$

The area of this surface section is

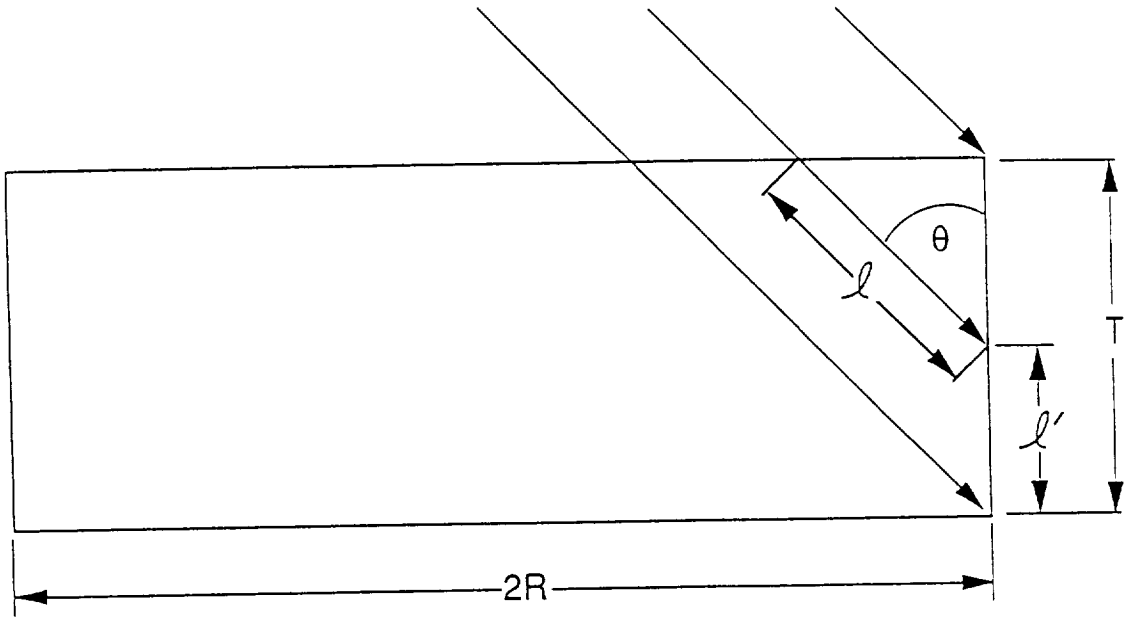

Figure 3. Illustration of group 2 trajectories when $0<\theta<\arctan(2R/T)$.

$$2R\ T\ (1 - L_{th}\ \cos\theta/L)\ .$$

The cross section is this area projected in the direction of the trajectory (if l' is positive, otherwise the cross section is zero) and we get:

$$\sigma_2(L,\theta) = \begin{cases} \text{If } 0 < \theta < \arctan(2R/T) \text{ then} \\ 2R\ T\ (1 - L_{th}\ \cos\theta/L)\ \sin\theta \quad \text{if } \cos\theta < L/L_{th} \\ 0 \quad \text{otherwise .} \end{cases}$$

Figure 4 illustrates group 2 trajectories for the case $\arctan(2R/T)<\theta<\pi/2$. SEUs are caused by the trajectories to the left of the one with length l (see Figure 4) satisfying (4) and such trajectories intersect a surface section of width l, (and area 2Rl') shown in the figure, where

$$l' = 2R - l\ \sin\theta = 2R - (L_{th}\ T/L)\ \sin\theta\ .$$

The area of this surface section is

$$2R\ (2R - L_{th}\ T\ \sin\theta/L)\ .$$

The cross section is this area projected in the direction of the trajectory (if l' is positive, otherwise the cross section is zero) and we get:

$$\sigma_2(L,\theta) = \begin{cases} \text{If } \arctan(2R/T) < \theta < \pi/2 \text{ then} \\ 2R\ (2R - L_{th}\ T\ \sin\theta/L)\ \cos\theta \quad \text{if } \sin\theta < 2RL/(T\ L_{th}) \\ 0 \quad \text{otherwise .} \end{cases}$$

Group 3 trajectories are similar to group 2 trajectories and the result is:

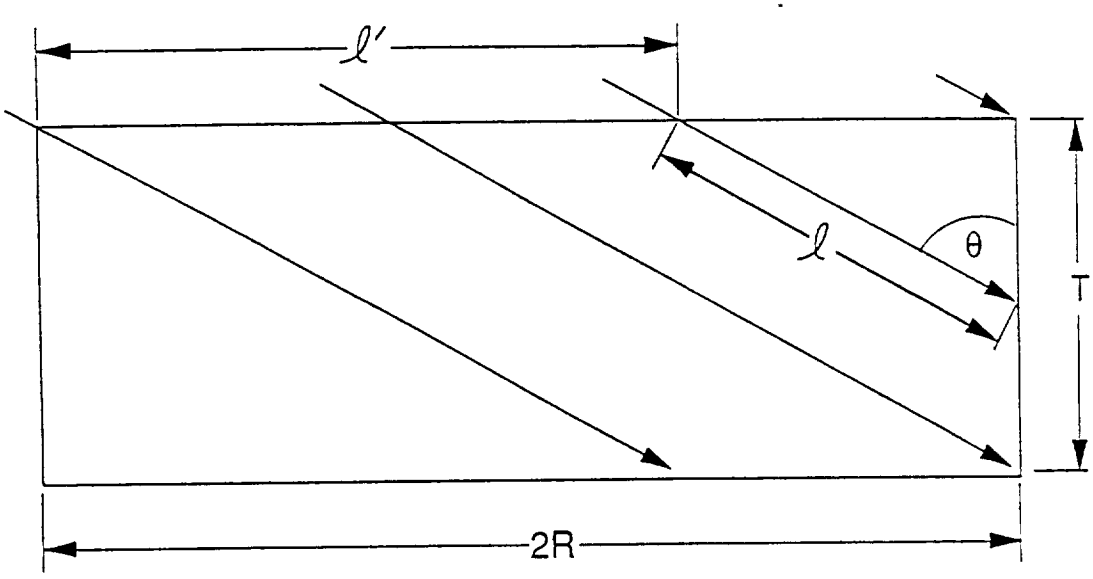

Figure 4. Illustration of group 2 trajectories when $\arctan(2R/T)<\theta<\pi/2$.

$$\text{If } 0 < \theta < \arctan(2R/T) \text{ then}$$

$$\sigma_3(L,\theta) = \begin{cases} 2R\ T\ (1 - L_{th}\ \cos\theta/L)\ \sin\theta & \text{if } \cos\theta < L/L_{th} \\ 0 & \text{otherwise .} \end{cases}$$

$$\text{If } \arctan(2R/T) < \theta < \pi/2 \text{ then}$$

$$\sigma_3(L,\theta) = \begin{cases} 2R\ (2R - L_{th}\ T\ \sin\theta/L)\ \cos\theta & \text{if } \sin\theta < 2RL/(T\ L_{th}) \\ 0 & \text{otherwise .} \end{cases}$$

The analysis for group 4 trajectories is similar to that for group 1 trajectories and the result is:

$$\text{If } 0 < \theta < \arctan(2R/T) \text{ then}$$

$$\sigma_4(L,\theta) = 0$$

$$\text{If } \arctan(2R/T) < \theta < \pi/2 \text{ then}$$

$$\sigma_4(L,\theta) = \begin{cases} 2R\ (T - 2R\ \cot\theta)\ \sin\theta & \text{if } \sin\theta < 2RL/(T\ L_{th}) \\ 0 & \text{otherwise .} \end{cases}$$

We next consider θ in the range $\pi/2<\theta<\pi$. For this range (representing particles moving upwards), the groups are redefined by interchanging upper and lower surfaces. It is evident that the partial cross sections for this range can be obtained from the previous expressions by replacing θ with $\pi-\theta$.

The symbolism can be shortened by using the unit step function δ_o (the subscript distinguishes it from a Dirac delta function) defined by

$$\delta_o(x) = \begin{cases} 1 \text{ if } x > 0 \\ 0 \text{ if } x \leq 0 . \end{cases}$$

The cross section is obtained by adding the partial cross sections and the result is:

$$\text{If } \quad 0 < \theta < \arctan(2R/T) \quad \text{then}$$
$$\sigma(L,\theta) = f(L,\cos\theta)\ \delta_o(L/L_{th} - \cos\theta)\ . \tag{5a}$$

$$\text{If } \quad \arctan(2R/T) < \theta < \pi/2 \quad \text{then}$$
$$\sigma(L,\theta) = f(L,\cos\theta)\ \delta_o(2R\ L/(T\ L_{th}) - \sin\theta). \tag{5b}$$

$$\text{If } \quad \pi/2 < \theta < \pi - \arctan(2R/T) \quad \text{then}$$
$$\sigma(L,\theta) = f(L,\cos(\pi-\theta))\ \delta_o(2R\ L/(T\ L_{th}) - \sin(\pi-\theta)). \tag{5c}$$

$$\text{If } \quad \pi - \arctan(2R/T) < \theta < \pi \quad \text{then}$$
$$\sigma(L,\theta) = f(L,\cos(\pi-\theta))\ \delta_o(L/L_{th} - \cos(\pi-\theta)) \tag{5d}$$

where f is defined by

$$f(L,\alpha)=4R^2\alpha+2RT(1-\alpha^2)^{1/2}-4RT(L_{th}/L)\alpha(1-\alpha^2)^{1/2} \quad \text{for } \alpha\epsilon[0,1]. \tag{6}$$

For future convenience, it is helpful to define S(L) by

$$S(L) = \text{sqrt*}(1 - 4R^2\ L^2/(T^2\ L_{th}^2)) \tag{7}$$

where the * indicates a modified square root function defined by

$$\text{sqrt*}(\alpha) = \begin{cases} \alpha^{1/2} & \text{if } \alpha \geq 0 \\ 0 & \text{if } \alpha < 0\ . \end{cases} \tag{8}$$

It is not difficult to show that

$$\delta_o(2R\ L/(T\ L_{th}) - \sin\theta) = \delta_o(\cos\theta - S(L)) \quad \text{for } \theta \in [0,\pi/2)$$

$$\delta_o(2R\ L/(T\ L_{th}) - \sin(\pi-\theta)) = \delta_o(\cos(\pi-\theta) - S(L)) \quad \text{for } \pi-\theta \in [0,\pi/2)$$

so that (5b) and (5c) can be written as

$$\text{If} \quad \arctan(2R/T) < \theta < \pi/2 \quad \text{then}$$
$$\sigma(L,\theta) = f(L,\cos\theta)\ \delta_o(\cos\theta - S(L)) \ . \tag{9a}$$

$$\text{If} \quad \pi/2 < \theta < \pi - \arctan(2R/T) \quad \text{then}$$
$$\sigma(L,\theta) = f(L,\cos(\pi-\theta))\ \delta_o(\cos(\pi-\theta) - S(L)) \ . \tag{9b}$$

Having evaluated σ, it is necessary to numerically evaluate the integral in (1). The ϕ integral can be carried out separately so that (1) can be written as

$$\text{rate} = 2\pi \int_0^\infty \int_0^\pi \sigma(L,\theta)\ h_a(L,\theta)\ \sin\theta\ d\theta\ dL \tag{10}$$

where

$$h_a(L,\theta) = (2\pi)^{-1} \int_0^{2\pi} h(L,\theta,\phi)\ d\phi \tag{11}$$

is the ϕ average of h.

The θ integration in (10) is carried out by partitioning the interval $[0,\pi)$ into the user specified subintervals

$$[a_i,a_{i+1}) \qquad i = 1, \ \ldots, \ N \ .$$

N and $a_1, \ \ldots, \ a_{N+1}$ are specified by the user but they must satisfy $0=a_1<a_2<\ldots<a_{N+1}=\pi$. The ϕ average flux, h_a, is treated as a constant (in θ) over each interval and h_{ai} denotes the flux for the i^{th} interval, i.e.,

$$h_{ai}(L) = h_a(L,\theta) \quad \text{for} \quad \theta \in [a_i,a_{i+1}) \ . \tag{12}$$

Another partitioning of $[0,\pi)$ consists of the intervals

$$[b_i, b_{i+1}) \qquad i = 1,\ 2,\ 3,\ 4$$

where

$$b_1 = 0 \tag{13a}$$

$$b_2 = \arctan(2R/T) \tag{13b}$$

$$b_3 = \pi/2 \tag{13c}$$

$$b_4 = \pi - \arctan(2R/T) \tag{13d}$$

$$b_5 = \pi \ . \tag{13e}$$

The interval $[0,\pi)$ can be expressed as the double union

$$[0,\pi) = \bigcup_{i=1}^{4} \bigcup_{j=1}^{N} C_{i,j} \tag{14}$$

where

$$C_{i,j} = [b_i, b_{i+1}) \cap [a_j, a_{j+1}) \ . \tag{15}$$

A more compact expression for $C_{i,j}$ can be obtained by defining

$$c^1_{i,j} = \max\{a_j, b_i\} \qquad i = 1,\ \ldots,\ 4 \qquad j = 1,\ \ldots,\ N \tag{16a}$$

$$c^2_{i,j} = \min\{a_{j+1}, b_{i+1}\} \qquad i = 1,\ \ldots,\ 4 \qquad j = 1,\ \ldots,\ N \tag{16b}$$

so that $C_{i,j}$ can be expressed as

$$C_{i,j} = \begin{cases} [c^1_{i,j},\ c^2_{i,j}) & \text{if } c^2_{i,j} > c^1_{i,j} \\ \text{empty} & \text{if } c^2_{i,j} \le c^1_{i,j} \ . \end{cases} \tag{17}$$

The $C_{i,j}$ intervals do not overlap (as seen by (15)) so any integral from 0 to π can be expressed as

$$\int_0^{\pi} = \sum_{j=1}^{N} \sum_{i=1}^{4} \int_{C_{i,j}} \tag{18}$$

where the integral on $C_{i,j}$ is defined by

$$\int_{C_{i,j}} = \int_{c^1_{i,j}}^{c^2_{i,j}} \quad \text{if } C_{i,j} \text{ is not empty}$$

$$\int_{C_{i,j}} = 0 \quad \text{if } C_{i,j} \text{ is empty}$$

and can be written more compactly as

$$\int_{C_{i,j}} = \delta_o(c^2_{i,j} - c^1_{i,j}) \int_{c^1_{i,j}}^{c^2_{i,j}} \; . \tag{19}$$

The θ integral in (10) can be evaluated using (12), (15), and (18) with the result

$$\int_0^{\pi} \sigma(L,\theta)\, h_a(L,\theta)\, \sin\theta\, d\theta = \sum_{j=1}^{N} h_{aj}(L) \sum_{i=1}^{4} \int_{C_{i,j}} \sigma(L,\theta)\, \sin\theta\, d\theta. \tag{20}$$

To evaluate the integrals on the right side of (20), use (19) and note that i=1 uses (5a), i=2 uses (9a), i=3 uses (9b), and i=4 uses (5d). The result is

$$\int_{C_{1,j}} \sigma(L,\theta)\, \sin\theta\, d\theta = \delta_o(c^2_{1,j} - c^1_{1,j}) \int_{D^2_{1,j}}^{D^1_{1,j}} f(L,z)\, \delta_o((L/L_{th}) - z)\, dz \tag{21a}$$

$$\int_{C_{2,j}} \sigma(L,\theta)\, \sin\theta\, d\theta = \delta_o(c^2_{2,j} - c^1_{2,j}) \int_{D^2_{2,j}}^{D^1_{2,j}} f(L,z)\, \delta_o(z - S(L))\, dz \tag{21b}$$

$$\int_{C_{3,j}} \sigma(L,\theta)\ \sin\theta\ d\theta = \delta_o(c^2{}_{3,j}-c^1{}_{3,j}) \int_{D^1_{3,j}}^{D^2_{3,j}} f(L,z)\ \delta_o(z-S(L))\ dz \qquad (21c)$$

$$\int_{C_{4,j}} \sigma(L,\theta)\ \sin\theta\ d\theta = \delta_o(c^2{}_{4,j}-c^1{}_{4,j}) \int_{D^1_{4,j}}^{D^2_{4,j}} f(L,z)\ \delta_o((L/L_{th})-z)\ dz \qquad (21d)$$

where the D's are defined by

$$D^k{}_{i,j} = \cos(c^k{}_{i,j}) \qquad \text{for } k = 1,2 \quad i = 1,2 \quad j = 1,\ldots,N \qquad (22a)$$

$$D^k{}_{i,j} = \cos(\pi - c^k{}_{i,j}) \qquad \text{for } k = 1,2 \quad i = 3,4 \quad j = 1,\ldots,N\ . \qquad (22b)$$

To evaluate the integrals in (21), define F by

$$F(L,z) = 2R^2\ z^2 + R\ T\ z\ (1-z^2)^{1/2} + R\ T\ \arcsin(z) + (4/3)R\ T\ (L_{th}/L)\ (1-z^2)^{3/2} \qquad \text{if } z \in [0,1] \qquad (23a)$$

$$F(L,z) = 0 \qquad \text{if } z < 0 \text{ or } z > 1 \qquad (23b)$$

so that F is an antiderivative (in z) of f. It is helpful to use the following identities, which are valid when $a,b \in [0,1]$:

$$\int_a^b f(L,z)\ \delta_o(c-z)\ dz = \delta_o(c-a)\ [F(L,c)-F(L,a)] + \delta_o(c-b)\ [F(L,b)-F(L,c)] \qquad (24a)$$

$$\int_a^b f(L,z)\ \delta_o(z-c)\ dz = \delta_o(a-c)\ [F(L,c)-F(L,a)] + \delta_o(b-c)\ [F(L,b)-F(L,c)]\ . \qquad (24b)$$

Note that if $c<0$ or $c>1$, F(L,c) is not defined in (23a) and, in order to avoid computer error, it is necessary to extend the domain of F. But $c<0$ or $c>1$ also implies that the F(L,c) terms drop out of the above equations so F(L,c) can be defined in any convenient way. This was the motivation for (23b), which extends

the domain of F in a particular convenient way.

Applying (24) to (21) gives

$$\int_{C_{1,j}} \sigma(L,\theta)\ \sin\theta\ d\theta =$$

$$\delta_o(c^2{}_{1,j}-c^1{}_{1,j})\ \delta_o((L/L_{th})-D^2{}_{1,j})\ [F^3(L)-F^2{}_{1,j}(L)]$$
$$+\ \delta_o(c^2{}_{1,j}-c^1{}_{1,j})\ \delta_o((L/L_{th})-D^1{}_{1,j})\ [F^1{}_{1,j}(L)-F^3(L)] \qquad (25a)$$

$$\int_{C_{2,j}} \sigma(L,\theta)\ \sin\theta\ d\theta =$$

$$\delta_o(c^2{}_{2,j}-c^1{}_{2,j})\ \delta_o(D^2{}_{2,j}-S(L))\ [F^4(L)-F^2{}_{2,j}(L)]$$
$$+\ \delta_o(c^2{}_{2,j}-c^1{}_{2,j})\ \delta_o(D^1{}_{2,j}-S(L))\ [F^1{}_{2,j}(L)-F^4(L)] \qquad (25b)$$

$$\int_{C_{3,j}} \sigma(L,\theta)\ \sin\theta\ d\theta =$$

$$\delta_o(c^2{}_{3,j}-c^1{}_{3,j})\ \delta_o(D^1{}_{3,j}-S(L))\ [F^4(L)-F^1{}_{3,j}(L)]$$
$$+\ \delta_o(c^2{}_{3,j}-c^1{}_{3,j})\ \delta_o(D^2{}_{3,j}-S(L))\ [F^2{}_{3,j}(L)-F^4(L)] \qquad (25c)$$

$$\int_{C_{4,j}} \sigma(L,\theta)\ \sin\theta\ d\theta =$$

$$\delta_o(c^2{}_{4,j}-c^1{}_{4,j})\ \delta_o((L/L_{th})-D^1{}_{4,j})\ [F^3(L)-F^1{}_{4,j}(L)]$$
$$+\ \delta_o(c^2{}_{4,j}-c^1{}_{4,j})\ \delta_o((L/L_{th})-D^2{}_{4,j})\ [F^2{}_{4,j}(L)-F^3(L)] \qquad (25d)$$

where the F arrays are defined by

$$F^1{}_{i,j}(L) = F(L, D^1{}_{i,j}) \tag{26a}$$

$$F^2{}_{i,j}(L) = F(L, D^2{}_{i,j}) \tag{26b}$$

$$F^3(L) = F(L, L/L_{th}) \tag{26c}$$

$$F^4(L) = F(L, S(L)) \ . \tag{26d}$$

Define the array $G_j(L)$ by

$$G_j(L) = \sum_{i=1}^{4} \int_{C_{i,j}} \sigma(L,\theta) \sin\theta \, d\theta \tag{27}$$

which can be expressed in terms of the F arrays via (25) and (27). Combining (10) with (20) and (27) gives

$$\text{rate} = 2\pi \sum_{j=1}^{N} \int_0^{\infty} h_{aj}(L) \, G_j(L) \, dL \ . \tag{28}$$

As an incidental point, we see from (28) that $2\pi G_j(L)$ is a cross section, associated with the j^{th} θ interval, for upsets for particles with LET equal to L. In an isotropic environment, the total effective cross section is

$$2\pi \sum_{j=1}^{N} G_j(L) \ .$$

This "effective cross section" is the quantity that the directional flux (in an isotropic environment consisting of particles all having the same LET L) must be multiplied by to produce the SEU rate. The cross section that the omnidirectional flux (directional flux times 4π) must be multiplied by to produce the rate is

$$(1/2) \sum_{j=1}^{N} G_j(L) \ .$$

To numerically integrate in LET, select LET values L_1, ..., L_M for some user specified M where L_1 is to be small enough so that the integral from 0 to L_1 is negligible (to avoid indeterminate forms, it is required that $L_1>0$) and L_M is to be large enough so that the integral from L_M to the largest possible particle LET is negligible. The rate is approximated by

$$\text{rate} = 2\pi \sum_{j=1}^{N} \sum_{k=1}^{M-1} \int_{L_k}^{L_{k+1}} h_{aj}(L) \ G_j(L) \ dL \ .$$

It is required that the L's be sufficiently closely spaced so that G_j is nearly a constant in each integral. This produces the approximation

$$\int_{L_k}^{L_{k+1}} h_{aj}(L) \ G_j(L) \ dL \approx$$

$$(1/2) \ [G_j(L_{k+1}) + G_j(L_k)] \int_{L_k}^{L_{k+1}} h_{aj}(L) \ dL =$$

$$(1/2)[G_j(L_{k+1}) + G_j(L_k)] \ [H_{aj}(L_k) - H_{aj}(L_{k+1})]$$

where H_{aj} is the integral (in LET) flux. The rate becomes

$$\text{rate} = \pi \sum_{j=1}^{N} \sum_{k=1}^{M-1} [G_{j,k+1} + G_{j,k}] \ [H_{aj,k} - H_{aj,k+1}] \qquad (29)$$

where

$$G_{j,k} = G_j(L_k) \qquad (30)$$

and $H_{aj,k}$ is a user supplied integral (in LET) directional flux evaluated at L_k and in the direction corresponding to the j^{th} θ interval and averaged in ϕ.

The equations needed for the actual computations are summarized below. The user supplies the L's. The b's are calculated from (13) and the a's are supplied by the user and are used to calculate the c's and D's via (16) and (22). The rate is calculated from (29) with $H_{aj,k}$ supplied by the user. $G_{j,k}$ is obtained by combining (30), (27), and (25) with the result

$$
\begin{aligned}
G_{j,k} = \\
&\delta_o(c^2_{1,j} - c^1_{1,j})\ \delta_o((L_k/L_{th}) - D^2_{1,j})\ [F^3_k - F^2_{1,j,k}] \\
&+ \delta_o(c^2_{1,j} - c^1_{1,j})\ \delta_o((L_k/L_{th}) - D^1_{1,j})\ [F^1_{1,j,k} - F^3_k] \\
&+ \delta_o(c^2_{2,j} - c^1_{2,j})\ \delta_o(D^2_{2,j} - S_k)\ [F^4_k - F^2_{2,j,k}] \\
&+ \delta_o(c^2_{2,j} - c^1_{2,j})\ \delta_o(D^1_{2,j} - S_k)\ [F^1_{2,j,k} - F^4_k] \\
&+ \delta_o(c^2_{3,j} - c^1_{3,j})\ \delta_o(D^1_{3,j} - S_k)\ [F^4_k - F^1_{3,j,k}] \\
&+ \delta_o(c^2_{3,j} - c^1_{3,j})\ \delta_o(D^2_{3,j} - S_k)\ [F^2_{3,j,k} - F^4_k] \\
&+ \delta_o(c^2_{4,j} - c^1_{4,j})\ \delta_o((L_k/L_{th}) - D^1_{4,j})\ [F^3_k - F^1_{4,j,k}] \\
&+ \delta_o(c^2_{4,j} - c^1_{4,j})\ \delta_o((L_k/L_{th}) - D^2_{4,j})\ [F^2_{4,j,k} - F^3_k] \qquad (31)
\end{aligned}
$$

where $S_k = S(L_k)$ and is evaluated from (7) with the result

$$S_k = \text{sqrt*}(1 - 4R^2\ L_k^2/(T^2\ L_{th}^2)) \qquad (32)$$

and $F^1_{i,j,k} = F^1_{i,j}(L_k)$, $F^2_{i,j,k} = F^2_{i,j}(L_k)$, $F^3_k = F^3(L_k)$, $F^4_k = F^4(L_k)$ and can be evaluated from (26) and (23) with the result

$$
\begin{aligned}
F^1_{i,j,k} &= 2R^2\ (D^1_{i,j})^2 + R\ T\ D^1_{i,j}\ (1 - (D^1_{i,j})^2)^{1/2} \\
&+ R\ T\ \arcsin(D^1_{i,j}) + (4/3)R\ T\ (L_{th}/L_k)\ (1 - (D^1_{i,j})^2)^{3/2} \\
&\qquad\qquad \text{for}\ \ l = 1,\ 2 \qquad (33a)
\end{aligned}
$$

$$
\begin{aligned}
F^3_k &= 2R^2\ (L_k/L_{th})^2 + R\ T\ (L_k/L_{th})\ (1 - (L_k/L_{th})^2)^{1/2} \\
&+ R\ T\ \arcsin(L_k/L_{th}) + (4/3)R\ T\ (L_{th}/L_k)\ (1 - (L_k/L_{th})^2)^{3/2} \\
&\qquad\qquad \text{if}\ \ L_k \le L_{th} \\
F^3_k &= 0 \qquad \text{if}\ \ L_k > L_{th} \qquad (33b)
\end{aligned}
$$

$$
\begin{aligned}
F^4_k &= 2R^2\ (S_k)^2 + R\ T\ S_k\ (1 - (S_k)^2)^{1/2} + R\ T\ \arcsin(S_k) \\
&\qquad + (4/3)R\ T\ (L_{th}/L_k)\ (1 - (S_k)^2)^{3/2}\ . \qquad (33c)
\end{aligned}
$$

6. PROGRAM NIFUR

The analysis in the last section is performed by the computer code NIFUR (NonIsotropic Flux Upset Rate) and the FORTRAN source code is listed in Appendix A.

Special compiling considerations may apply if the code is modified by changing the DIMENSION statements. This discussion uses terminology applicable to IBM PCs using the Microsoft FORTRAN Compiler with the large memory model. There is a potential problem (if modifications are made) due to the large memory reserved for the arrays. The arrays will not all fit in the default data segment and must be placed elsewhere. As the code is written, this placement is automatic because the largest arrays exceed 64K and the default procedure is to give them huge addresses and place them outside the default data segment. The second largest arrays exceed the default data threshold (32K) and are automatically placed outside the default data segment. The remaining arrays fit in the default data segment. The problem occurs if the array sizes are reduced (by editing the DIMENSION statements) in such a way that the placement is not automatic but still required because the arrays total to more than 64K. In this case, we must request the placement when the code is compiled. This is done using the Gt option (applicable to the Microsoft compiler). Specifically, the code is compiled with the command "FL/Gt NIFUR.FOR" (the Gt option is not needed if the code is not modified). If a different compiler is used, it is up to the user to determine the equivalent option applicable to that compiler (if such an option is needed). The compiled code should be tested against the example in Section 10 to verify that it is working properly.

The code requires input files which are created the following way. The θ interval $[0,\pi)$ is divided up into user selected subintervals and the directional flux is treated as constant (in the θ coordinate) on each subinterval. The user supplies a separate

table for each θ interval, which tabulates flux against LET (the smallest LET value used in the flux tabulation must be greater than zero). An input file HFLUX00.DAT must be created, which identifies the θ intervals and LET values to be used in the flux tables. Another input file, HFLUX01.DAT, must be created, which lists the flux as a function of LET for the first θ interval (LET values are not listed in this file because they are in HFLUX00.DAT). Similarly, HFLUX02.DAT contains the flux for the second θ interval, etc. The flux is required to be a directional (corresponding to the appropriate θ interval) integral in LET flux which is averaged in the ϕ coordinate. The input file formats are described in detail in the source code comment statements. If there is confusion, the example in Section 10 might help. Device data (A, T, and L_{th}) are entered via prompts and the code output (the upper bound SEU rate estimate) is displayed on the terminal.

In the special case of an isotropic flux, SEU rates for box-shaped, charge-collecting volumes can be calculated from the chord length distribution function for a box [3], and it is interesting to compare this exact calculation to NIFUR results. Suppose an area A is used in the NIFUR calculation while the exact chord length distribution calculation is performed for a box with both lateral dimensions equal to $A^{1/2}$ (L_{th} and T are the same for both calculations). If T is sufficiently small, the NIFUR calculated SEU rate will be about $4/\pi$ or about 1.27 times the chord length distribution calculated rate. The reason is that, for small T, the rate is proportional to A. Although NIFUR is given the area A, which is assigned to a circular-cylindrical volume, the area it actually calculates with is the normal incident area of the rotating box, which is $4A/\pi$. Hence, the two calculations disagree by a factor of 1.27 (if T is not small, the exact relation between the two calculations is not simple, although they are roughly equal). If desired, the NIFUR results can be modified by dividing by 1.27. If this is done, we cannot rigorously conclude (from the analysis given here) that the

modified rate is an upper bound estimate, but it is "probably" an upper bound (at least it is nearly equal to an upper bound) and it will conform better (for small T) to more exact calculations.

7. EFFECTIVE FLUX

In this section, we confine our attention to hypothetical or real devices with the property that the normal incident cross section versus LET curve can be approximated by a step function. The normal incident behavior of such devices is characterized by two parameters; a threshold LET, L_{th}, and a cross sectional area, A. The "maximized rate" in a given three dimensional environment is defined as the rate predicted by NIFUR with thickness, T, chosen to maximize the rate. If a device contains a single circular-cylindrical, charge-collecting volume, it is evident that the maximized rate is an upper bound for the actual SEU rate because it was constructed to be such.

It is, perhaps, less obvious that the maximized rate (calculated from L_{th} and A) is also an upper bound for the SEU rate of a device containing any number of identical or nonidentical circular-cylindrical, charge-collecting volumes, all having the same L_{th} and with normal incident areas totaling to A. This is true for the following reason. Suppose a device contains a collection of such volumes, and the thickness of each volume is selected to produce a maximum rate for that volume. The sum of the rates for each volume is an upper bound for the device SEU rate. It can be shown that this choice of thicknesses will result in all volumes being geometrically similar. But for geometrically similar volumes with the same threshold LET, the rates predicted by NIFUR are proportional to the normal incident areas, and the sum of the rates (an upper bound for the device rate) is the same as the

rate for a single volume of normal incident area A[1] (which is the maximized rate). Hence, the maximized rate is an upper bound whether the device contains one, or many, identical or nonidentical circular-cylindrical volumes all having the same threshold LET.

From the above discussion, it is reasonable to expect that the maximized rate, for a given A and L_{th}, is an upper bound for the SEU rate of any device having the same A and L_{th}. The maximized rate is proportional to A and a normalized rate can be obtained by dividing the maximized rate by A. This normalized rate, which depends (for a fixed environment) only on L_{th}, will be called the "effective flux" evaluated at LET=L_{th}. The effective flux evaluated at LET=L_{th} and multiplied by A is an upper bound for the SEU rate for any device with threshold LET L_{th} and cross section A.

In summary:

1. Effective flux evaluated at a given LET is constructed by running NIFUR with L_{th} equal to the given LET value and selecting an arbitrary A. T is varied to produce a maximum rate and the effective flux is this maximum rate divided by A.

2. If a tabulation of effective flux versus LET is available, an upper bound SEU rate estimate for a device with threshold LET L_{th} and cross section A can be obtained by evaluating the effective flux at LET=L_{th} and multiplying it by A.

1.For example, 10^8 cylinders with radius and thickness equal to 1 μm produce the same SEU rate as one cylinder with radius and thickness equal to 1 cm. The fact that the one large cylinder is nonphysical (the dimensions are much larger than those of any physical structures) is irrelevant.

8. PROGRAM EFFLUX

Upper bound SEU rate estimates are trivial if a tabulation of effective flux is available. The only calculation that requires any work is the construction of the effective flux which is done by the EFFLUX code.

The FORTRAN source code is listed in Appendix B. The same compiling considerations applicable to NIFUR apply to this code (see Section 6) and the compiled code should be tested against the example in Section 10 to verify that it is working properly.

This program is the same as NIFUR except that the user does not specify values for L_{th}, A, or T. Values are automatically assigned as discussed in the last section. The input files are the same as those used by NIFUR and the output is an effective flux tabulation which will be in the file EFFLUX.OUT.

EFFLUX tabulates effective flux against the same LET values that the original, user specified, flux was tabulated against. However, the effective flux is meaningless (and should not be used for SEU rate calculations) at the smallest LET values. The reason is that a device with threshold LET equal to the smallest tabulated LET value can be upset from particles with a smaller LET, and such particles are not included in the original flux table (their LETs are below the tabulated range). The effective flux is not meaningful unless it is evaluated at a LET that is one or more orders of magnitude greater than the smallest LET in the user supplied flux tabulation. If a device has a small threshold LET, so that the effective flux must be evaluated at a small LET, the user supplied flux tabulation must extend to very small LET values.

As discussed in Section 6, it might be desirable to modify the effective flux by dividing it by 1.27. It was not rigorously shown that rate estimates obtained from such a modified flux are

upper bounds for actual rates, but this is a minor modification (compared to other sources of error) and will produce better conformity with other rate calculation methods.

9. DEVICES WITH SMOOTH CROSS SECTION VERSUS LET CURVES

Until now it was assumed that a normal incident device cross section versus LET curve is a step function. Effective flux can also be used to calculate upper bound SEU rates for smooth cross section curves. For a smooth curve, the device is modeled as consisting of a collection of charge-collecting volumes which do not have the same threshold LET.

Suppose two devices each contain a collection of circular-cylindrical, charge-collecting volumes and, at every LET, the normal incident device cross section (sum of the step functions associated with individual volumes) of the first device is greater than or equal to that of the second device. There need not be any relationship between the volumes in the two devices, other than the condition that one cross section curve bounds the other. It can be shown that the upper bound SEU rate for the first device (obtain by using the method of Section 7 for each charge-collecting volume and adding rates) is also an upper bound for the second device[1]. This implies that if we are given a cross section curve for a device containing an unknown collection of charge-collecting volumes, an upper bound rate estimate can be obtained by calculating the upper bound rate for any convenient hypothetical device having a cross section curve that bounds the given curve. In particular, if we are given a smooth curve, such as the one in Figure 5, we can construct a staircase curve which

---

1.This intuitively obvious statement can be proven rigorously, but the proof is too long to include here.

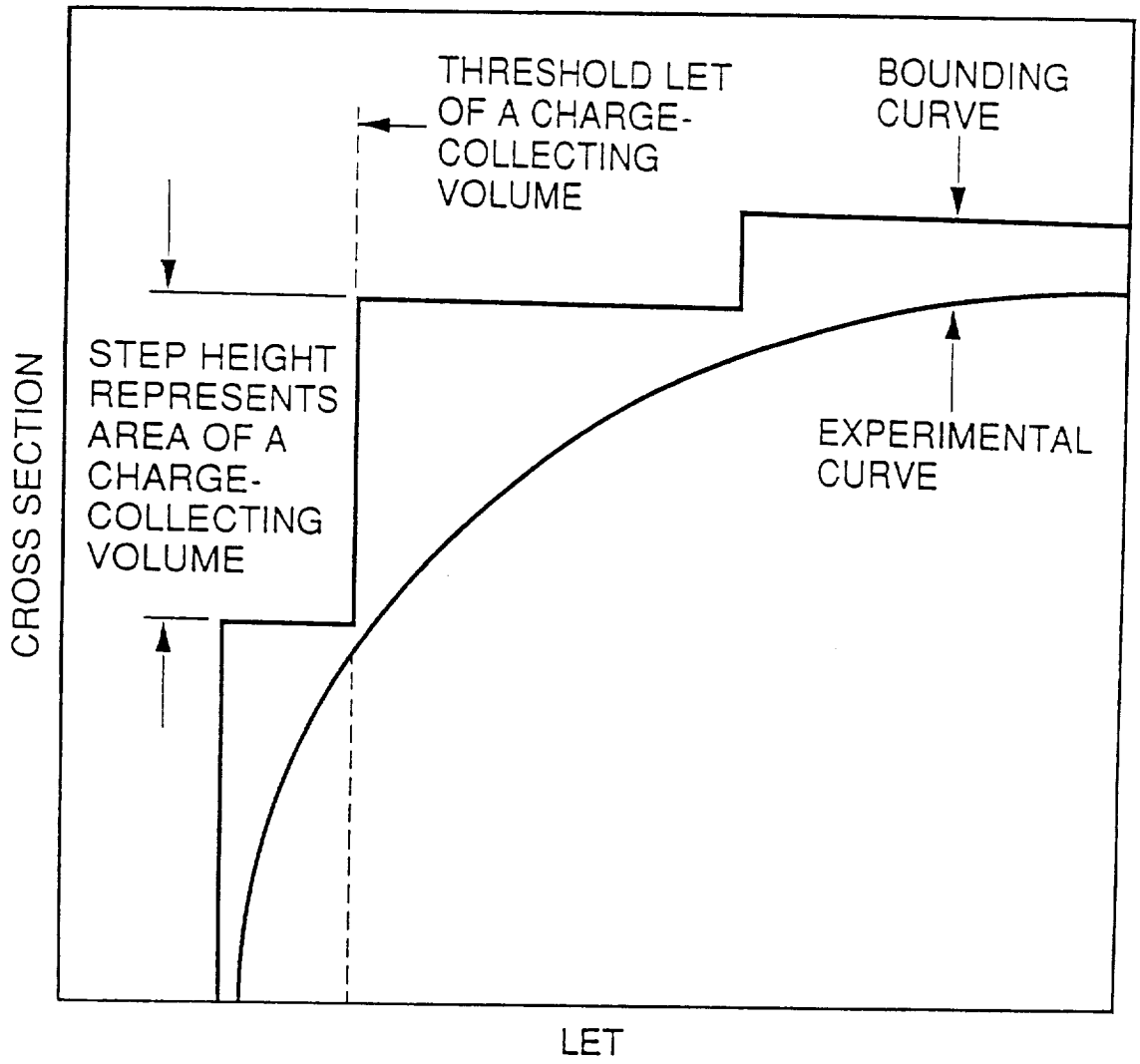

Figure 5. An experimental device cross section versus LET curve and a staircase curve that bounds it.

bounds the given curve, but is otherwise arbitrary. The staircase curve represents a hypothetical device which contains one charge-collecting volume for each step in the staircase. The normal incident area of a given volume is the height of the step associated with that volume and the threshold LET of the volume is the LET coordinate of the step (see Figure 5). After finding the area and threshold LET of each volume, an upper bound rate is obtained for each volume using the method of Section 7 and the rates are added to produce an upper bound estimate for the actual device. An example is given in the next section to illustrate this algorithm.

It is significant that the steps in the staircase curve do not have to correspond to physical structures of the actual device. Any staircase function that bounds the cross section curve can be used, but the lowest (most accurate) upper bound estimates are produced by the curves that conform most closely to the actual curve.

As an incidental point, the above algorithm has the mathematical interpretation of a numerical integration. The algorithm produces an upper bound for the integral

$$\int EF(L)\ dX(L)$$

where EF(L) is the effective flux evaluated at LET=L and X(L) is the normal incident device cross section evaluated at LET=L. The limiting case of an infinitely fine division (the staircase curve has an infinite number of steps and conforms to the actual curve) produces the integral exactly. It is not necessary to be aware of this in order to perform the calculations, but this information is helpful when looking for similarities between the SEU rate prediction method discussed here and other methods reported in the literature.

10. AN EXAMPLE

The example below estimates the SEU rate for a hypothetical device in a hypothetical spacecraft exposed to a hypothetical solar flare.

The mass distribution, relative to the device orientation, in this hypothetical spacecraft requires that a different shield thickness be used to calculate the flux for each of the angular regions shown below:

Region 1:	$0 < \theta < 45°$,	$0 < \phi < 360°$
Region 2:	$45° < \theta < 75°$,	$\phi < 45°$ or $\phi > 315°$
Region 3:	$45° < \theta < 75°$,	$45° < \phi < 135°$
Region 4:	$45° < \theta < 75°$,	$135° < \phi < 225°$
Region 5:	$45° < \theta < 75°$,	$225° < \phi < 315°$
Region 6:	$75° < \theta < 90°$,	$45° < \phi < 135°$
Region 7:	$75° < \theta < 90°$,	$\phi < 45°$ or $\phi > 315°$
Region 8:	$75° < \theta < 90°$,	$225° < \phi < 315°$
Region 9:	$75° < \theta < 90°$,	$135° < \phi < 225°$
Region 10:	$90° < \theta < 180°$,	$0 < \phi < 360°$

where θ is measured from the device normal and ϕ is measured from some line lying in the device plane.

The Heinrich flux behind the shield thicknesses associated with each angular region is calculated by a computer code such as CREME [1]. A particular code, using a particular (and severe) solar flare model and particular shield thicknesses produced the flux tables shown in Table 1[1].

1.This calculation is not discussed in detail here because the user must use his own resources (e.g., CREME [1]) to obtain these flux tables. The present discussion is concerned with what to do with the tables, not how to get them.

LET	REGION 1 FLUX	REGION 2 FLUX	REGION 3 FLUX	REGION 4 FLUX	REGION 5 FLUX
.1000E+0	.237E+6	.134E+6	.182E+7	.325E+6	.224E+6
.1259E+0	.161E+6	.969E+5	.117E+7	.218E+6	.153E+6
.1585E+0	.113E+6	.708E+5	.757E+6	.147E+6	.106E+6
.1995E+0	.790E+5	.525E+5	.472E+6	.100E+6	.750E+5
.2512E+0	.567E+5	.396E+5	.303E+6	.703E+5	.544E+5
.3162E+0	.418E+5	.300E+5	.206E+6	.511E+5	.403E+5
.3981E+0	.299E+5	.222E+5	.132E+6	.357E+5	.290E+5
.5012E+0	.217E+5	.169E+5	.813E+5	.253E+5	.212E+5
.6310E+0	.180E+5	.142E+5	.640E+5	.207E+5	.177E+5
.7943E+0	.152E+5	.120E+5	.497E+5	.172E+5	.149E+5
.1000E+1	.135E+5	.108E+5	.403E+5	.150E+5	.132E+5
.1259E+1	.964E+4	.755E+4	.286E+5	.108E+5	.951E+4
.1585E+1	.660E+4	.511E+4	.203E+5	.741E+4	.650E+4
.1995E+1	.399E+4	.303E+4	.136E+5	.449E+4	.392E+4
.2512E+1	.256E+4	.192E+4	.974E+4	.291E+4	.251E+4
.3162E+1	.179E+4	.131E+4	.726E+4	.204E+4	.175E+4
.3981E+1	.908E+3	.638E+3	.472E+4	.101E+4	.898E+3
.5012E+1	.663E+3	.464E+3	.354E+4	.727E+3	.654E+3
.6310E+1	.351E+3	.245E+3	.216E+4	.385E+3	.346E+3
.7943E+1	.203E+3	.142E+3	.130E+4	.222E+3	.202E+3
.1000E+2	.121E+3	.850E+2	.798E+3	.132E+3	.121E+3
.1259E+2	.807E+2	.571E+2	.529E+3	.880E+2	.806E+2
.1585E+2	.218E+2	.156E+2	.145E+3	.238E+2	.217E+2
.1995E+2	.110E+2	.787E+1	.726E+2	.120E+2	.110E+2
.2512E+2	.380E+1	.270E+1	.248E+2	.414E+1	.379E+1
.3162E+2	.895E-1	.559E-1	.354E+0	.106E+0	.882E-1
.3981E+2	.323E-1	.188E-1	.107E+0	.395E-1	.316E-1
.5012E+2	.159E-1	.892E-2	.516E-1	.197E-1	.153E-1
.6310E+2	.642E-2	.352E-2	.208E-1	.799E-2	.625E-2
.7943E+2	.240E-2	.129E-2	.771E-2	.299E-2	.237E-2
.1000E+3	.829E-4	.425E-4	.285E-3	.980E-4	.819E-4

Table 1. Integral directional Heinrich flux versus LET for each angular region. LET in units of MeV-cm^2/mg and flux in units of particles/m^2-sec-sr.

LET	REGION 6 FLUX	REGION 7 FLUX	REGION 8 FLUX	REGION 9 FLUX	REGION10 FLUX
.1000E+0	.182E+7	.372E+6	.978E+6	.102E+6	.362E+6
.1259E+0	.117E+7	.244E+6	.620E+6	.763E+5	.237E+6
.1585E+0	.757E+6	.164E+6	.400E+6	.572E+5	.160E+6
.1995E+0	.472E+6	.111E+6	.257E+6	.434E+5	.109E+6
.2512E+0	.303E+6	.775E+5	.169E+6	.333E+5	.761E+5
.3162E+0	.206E+6	.561E+5	.117E+6	.255E+5	.549E+5
.3981E+0	.132E+6	.391E+5	.775E+5	.190E+5	.381E+5
.5012E+0	.813E+5	.276E+5	.500E+5	.145E+5	.268E+5
.6310E+0	.640E+5	.225E+5	.399E+5	.122E+5	.218E+5
.7943E+0	.497E+5	.186E+5	.315E+5	.104E+5	.181E+5
.1000E+1	.403E+5	.162E+5	.261E+5	.931E+4	.157E+5
.1259E+1	.286E+5	.117E+5	.186E+5	.645E+4	.113E+5
.1585E+1	.203E+5	.802E+4	.130E+5	.431E+4	.777E+4
.1995E+1	.136E+5	.487E+4	.828E+4	.254E+4	.472E+4
.2512E+1	.974E+4	.318E+4	.563E+4	.160E+4	.308E+4
.3162E+1	.726E+4	.219E+4	.399E+4	.109E+4	.213E+4
.3981E+1	.472E+4	.108E+4	.228E+4	.542E+3	.105E+4
.5012E+1	.354E+4	.778E+3	.164E+4	.400E+3	.759E+3
.6310E+1	.216E+4	.413E+3	.962E+3	.214E+3	.402E+3
.7943E+1	.130E+4	.236E+3	.579E+3	.124E+3	.231E+3
.1000E+2	.798E+3	.141E+3	.351E+3	.737E+2	.137E+3
.1259E+2	.529E+3	.932E+2	.238E+3	.492E+2	.908E+2
.1585E+2	.145E+3	.252E+2	.635E+2	.132E+2	.246E+2
.1995E+2	.726E+2	.127E+2	.319E+2	.667E+1	.124E+2
.2512E+2	.248E+2	.438E+1	.109E+2	.228E+1	.427E+1
.3162E+2	.354E+0	.118E+0	.191E+0	.401E-1	.114E+0
.3981E+2	.107E+0	.446E-1	.721E-1	.130E-1	.429E-1
.5012E+2	.516E-1	.220E-1	.353E-1	.622E-2	.209E-1
.6310E+2	.208E-1	.897E-2	.144E-1	.249E-2	.862E-2
.7943E+2	.771E-2	.341E-2	.540E-2	.915E-3	.329E-2
.1000E+3	.285E-3	.123E-3	.199E-3	.301E-4	.117E-3

Table 1. (continued)

For each θ interval, the fluxes must be averaged in ϕ. For each θ interval, each ϕ interval is the same size so a ϕ average is a simple numerical average (if the ϕ intervals were not the same size, the fluxes would be weighted according to the sizes of the ϕ intervals in the obvious way). The Region 1 flux is the ϕ average flux for the θ interval (0,45°) and the Region 10 flux is the ϕ average flux for the θ interval (90°,180°). The fluxes for Regions 2,3,4, and 5 are averaged to produce the ϕ average flux for the θ interval (45°,75°) and the fluxes for Regions 6,7,8, and 9 are averaged to produce the ϕ average flux for the θ interval (75°,90°). This averaging is a lot of work if done by hand (especially if the ϕ intervals are not uniform and a weighted average is required) and the user will probably want to write a code that will speed this up. The averaged fluxes for our example are shown in Table 2. This table is used to produce the input files used by EFFLUX as described in the code comment statements. The input files are shown in Table 3.

Before proceeding, this is a good time to test NIFUR. If NIFUR is run with the Table 3 files together with $A=10^{-6}$, $L_{th}=5$, and $T=10^{-4}$, it should respond with RATE=.282754.

The next step is to run EFFLUX. The output of EFFLUX is the effective flux and is shown in Table 4. Because the smallest LET in the original flux tabulation is 0.1 MeV-cm^2/mg, the effective flux tabulation should not be trusted for LET less than 1 MeV-cm^2/mg (see Section 8). Discarding the lower LET entries and dividing the flux by 1.27 (as suggested in Section 8) produces the final effective flux table which is shown in Table 5.

Now that the effective flux has been calculated, the next step is to estimate the SEU rate. In this example, the device is represented by the following cross section data:

LET	0<θ<45° FLUX	45°<θ<75° FLUX	75°<θ<90° FLUX	90°<θ<180° FLUX
.1000E+0	.237E+6	.626E+6	.818E+6	.362E+6
.1259E+0	.161E+6	.409E+6	.528E+6	.237E+6
.1585E+0	.113E+6	.270E+6	.345E+6	.160E+6
.1995E+0	.790E+5	.175E+6	.221E+6	.109E+6
.2512E+0	.567E+5	.117E+6	.146E+6	.761E+5
.3162E+0	.418E+5	.819E+5	.101E+6	.549E+5
.3981E+0	.299E+5	.547E+5	.669E+5	.381E+5
.5012E+0	.217E+5	.362E+5	.434E+5	.268E+5
.6310E+0	.180E+5	.292E+5	.347E+5	.218E+5
.7943E+0	.152E+5	.235E+5	.276E+5	.181E+5
.1000E+1	.135E+5	.198E+5	.230E+5	.157E+5
.1259E+1	.964E+4	.141E+5	.163E+5	.113E+5
.1585E+1	.660E+4	.983E+4	.114E+5	.777E+4
.1995E+1	.399E+4	.626E+4	.732E+4	.472E+4
.2512E+1	.256E+4	.427E+4	.504E+4	.308E+4
.3162E+1	.179E+4	.309E+4	.363E+4	.213E+4
.3981E+1	.908E+3	.182E+4	.216E+4	.105E+4
.5012E+1	.663E+3	.135E+4	.159E+4	.759E+3
.6310E+1	.351E+3	.784E+3	.937E+3	.402E+3
.7943E+1	.203E+3	.467E+3	.560E+3	.231E+3
.1000E+2	.121E+3	.284E+3	.341E+3	.137E+3
.1259E+2	.807E+2	.189E+3	.227E+3	.908E+2
.1585E+2	.218E+2	.515E+2	.617E+2	.246E+2
.1995E+2	.110E+2	.259E+2	.310E+2	.124E+2
.2512E+2	.380E+1	.886E+1	.106E+2	.427E+1
.3162E+2	.895E-1	.151E+0	.176E+0	.114E+0
.3981E+2	.323E-1	.492E-1	.592E-1	.429E-1
.5012E+2	.159E-1	.239E-1	.288E-1	.209E-1
.6310E+2	.642E-2	.964E-2	.117E-1	.862E-2
.7943E+2	.240E-2	.359E-2	.436E-2	.329E-2
.1000E+3	.829E-4	.127E-3	.159E-3	.117E-3

Table 2. ϕ average of the Table 1 fluxes for the four θ intervals. The units are the same as in Table 1.

HFLUX00.DAT	HFLUX01.DAT	HFLUX02.DAT	HFLUX03.DAT	HFLUX04.DAT
4	.237E+06	.626E+06	.818E+06	.362E+06
31	.161E+06	.409E+06	.528E+06	.237E+06
45.0	.113E+06	.270E+06	.345E+06	.160E+06
75.0	.790E+05	.175E+06	.221E+06	.109E+06
90.0	.567E+05	.117E+06	.146E+06	.761E+05
.1000E+00	.418E+05	.819E+05	.101E+06	.549E+05
.1259E+00	.299E+05	.547E+05	.669E+05	.381E+05
.1585E+00	.217E+05	.362E+05	.434E+05	.268E+05
.1995E+00	.180E+05	.292E+05	.347E+05	.218E+05
.2512E+00	.152E+05	.235E+05	.276E+05	.181E+05
.3162E+00	.135E+05	.198E+05	.230E+05	.157E+05
.3981E+00	.964E+04	.141E+05	.163E+05	.113E+05
.5012E+00	.660E+04	.983E+04	.114E+05	.777E+04
.6310E+00	.399E+04	.626E+04	.732E+04	.472E+04
.7943E+00	.256E+04	.427E+04	.504E+04	.308E+04
.1000E+01	.179E+04	.309E+04	.363E+04	.213E+04
.1259E+01	.908E+03	.182E+04	.216E+04	.105E+04
.1585E+01	.663E+03	.135E+04	.159E+04	.759E+03
.1995E+01	.351E+03	.784E+03	.937E+03	.402E+03
.2512E+01	.203E+03	.467E+03	.560E+03	.231E+03
.3162E+01	.121E+03	.284E+03	.341E+03	.137E+03
.3981E+01	.807E+02	.189E+03	.227E+03	.908E+02
.5012E+01	.218E+02	.515E+02	.617E+02	.246E+02
.6310E+01	.110E+02	.259E+02	.310E+02	.124E+02
.7943E+01	.380E+01	.886E+01	.106E+02	.427E+01
.1000E+02	.895E-01	.151E+00	.176E+00	.114E+00
.1259E+02	.323E-01	.492E-01	.592E-01	.429E-01
.1585E+02	.159E-01	.239E-01	.288E-01	.209E-01
.1995E+02	.642E-02	.964E-02	.117E-01	.862E-02
.2512E+02	.240E-02	.359E-02	.436E-02	.329E-02
.3162E+02	.829E-04	.127E-03	.159E-03	.117E-03
.3981E+02				
.5012E+02				
.6310E+02				
.7943E+02				
.1000E+03				

Table 3. Input files. The file names at the top are not part of the file contents.

EFFECTIVE FLUX

LET IN UNITS OF MeV-cm**2/mg
FLUX IN UNITS OF 1/(cm**2-day)

LET	FLUX
0.1000E+00	0.5248E+08
0.1259E+00	0.4234E+08
0.1585E+00	0.3263E+08
0.1995E+00	0.2487E+08
0.2512E+00	0.1865E+08
0.3162E+00	0.1387E+08
0.3981E+00	0.1024E+08
0.5012E+00	0.7514E+07
0.6310E+00	0.5511E+07
0.7943E+00	0.4078E+07
0.1000E+01	0.3064E+07
0.1259E+01	0.2318E+07
0.1585E+01	0.1735E+07
0.1995E+01	0.1276E+07
0.2512E+01	0.9207E+06
0.3162E+01	0.6598E+06
0.3981E+01	0.4672E+06
0.5012E+01	0.3264E+06
0.6310E+01	0.2271E+06
0.7943E+01	0.1561E+06
0.1000E+02	0.1064E+06
0.1259E+02	0.7171E+05
0.1585E+02	0.4733E+05
0.1995E+02	0.3071E+05
0.2512E+02	0.1969E+05
0.3162E+02	0.1249E+05
0.3981E+02	0.7847E+04
0.5012E+02	0.4902E+04
0.6310E+02	0.3058E+04
0.7943E+02	0.1909E+04
0.1000E+03	0.1188E+04

Table 4. Contents of the file EFFLUX.OUT.

EFFECTIVE FLUX

LET IN UNITS OF MeV-cm**2/mg
FLUX IN UNITS OF 1/(cm**2-day)

LET	FLUX
0.1000E+01	0.241E+07
0.1259E+01	0.183E+07
0.1585E+01	0.137E+07
0.1995E+01	0.100E+07
0.2512E+01	0.725E+06
0.3162E+01	0.520E+06
0.3981E+01	0.368E+06
0.5012E+01	0.257E+06
0.6310E+01	0.179E+06
0.7943E+01	0.123E+06
0.1000E+02	0.838E+05
0.1259E+02	0.565E+05
0.1585E+02	0.373E+05
0.1995E+02	0.242E+05
0.2512E+02	0.155E+05
0.3162E+02	0.983E+04
0.3981E+02	0.618E+04
0.5012E+02	0.386E+04
0.6310E+02	0.241E+04
0.7943E+02	0.150E+04
0.1000E+03	0.935E+03

Table 5. The final effective flux table.

Cross section (cm^2)	LET (MeV-cm^2/mg)
Approximately zero	3
9.2×10^{-4}	6
5.7×10^{-3}	16
1.6×10^{-2}	$\geq$ 40

A staircase function is constructed to bound the cross section curve as illustrated in Figure 5. The vertices are arbitrary and in this example are chosen to correspond to the discrete points listed above. Each step in the staircase function defines a cross section and threshold LET for a hypothetical charge-collecting volume as listed below (note that a given cross section corresponds to a smaller LET than in the original data, e.g., 9.2×10^{-4} corresponds to 3 instead of 6). Also listed are the approximate effective fluxes evaluated at the LETs. Upset rate estimates are constructed from this data as shown (the obvious units are implied).

Charge-collecting volume #	Cross section	Threshold LET	Effective flux
1	9.2×10^{-4}	3	5.7×10^{5}
2	5.7×10^{-3} -9.2×10^{-4} $=4.8 \times 10^{-3}$	6	2.0×10^{5}
3	1.6×10^{-2} -5.7×10^{-3} $=1.0 \times 10^{-2}$	16	3.7×10^{4}

Upper bound SEU rate =

$$(9.2 \times 10^{-4})(5.7 \times 10^{5}) + (4.8 \times 10^{-3})(2.0 \times 10^{5}) + (1.0 \times 10^{-2})(3.7 \times 10^{4})$$

$$= 1.9 \times 10^{3}/\text{day}.$$

11. CONCLUSION

The analysis given here provides a way to standardize SEU rate calculations for a given space mission. The proposed method is the following: The flight project is required to estimate the environments of concern (e.g., typical flux, peak flux, mission integrated fluence, etc.) with the effects of mass shielding included. Using the computer code EFFLUX, the flight project constructs tables of effective flux versus LET. If the environment must be treated as nonisotropic, different tables are needed for different device orientations relative to the spacecraft. A device vendor can then calculate SEU rates by using a simple numerical integration to combine device cross section data with the effective flux tables.

The purpose of the effective flux is to simplify SEU rate calculations from the vendor's point of view. Most of the work required for SEU rate estimates is performed by the flight project when constructing effective flux tables. After these tables have been constructed, SEU rate estimates are simple.

```
      PROGRAM NIFUR
C Copyright (c) 1991, California Institute of Technology.
C U.S. Government Sponsorship under NASA Contract NAS7-918
C is acknowledged.
      REAL LTH,L(200)
      CHARACTER*2,FLNM1
      CHARACTER*11,FLNM2
      DIMENSION A(31),B(5),C1(4,30),C2(4,30),D1(4,30),D2(4,30)
      DIMENSION S(200),HA(30,200)
      DIMENSION F3(200),F4(200),F1(4,30,200),F2(4,30,200)
      DIMENSION G(30,200)
C Read data. Device data consists of a normal incident cross
C section AC, a threshold LET LTH, and a thickness T, which
C are entered via prompts. The files HFLUX00.DAT, HFLUX01.DAT,
C ..., HFLUX09.DAT, HFLUX10.DAT, HFLUX11.DAT, ... contain
C environmental data. There is one file (after the "00" file)
C for each angular bin (discussed below). The angular inter-
C val [0,180 degrees) is partitioned into the bins
C [A(1),A(2)), [A(2),A(3)), ...,[A(N),A(N+1)) where A(1)=0
C and A(N+1)=180. The discrete values L(1), ...,L(M) of LET
C (in MeV-cm**2/mg) are selected by the user. The file
C HFLUX00.DAT contains the values of N, M, A(2), ..., A(N),
C L(1), ..., L(M) respectively. (Note that the A's are read
C in degrees and then converted into radians. Also note that,
C for an isotropic flux, N=1 and no A's are listed in
C HFLUX00.DAT.) The file HFLUX01.DAT contains the values of
C HA(1,1), HA(1,2), ..., HA(1,M) where HA(J,K) is the integral
C (in LET) directional flux ( in 1/m**2-sec-sr) evaluated at
C LET=L(K) and in the direction corresponding to the JTH
C angular bin. Etc. for the other files. Note that N must
C not exceed 30 and M must not exceed 200. After reading HA,
C convert to the units 1/cm**2-day-sr.
      PI=ATAN2(0.0,-1.0)
      PI2=ATAN2(1.0,0.0)
      WRITE(*,*)'ENTER NORMAL INCIDENT CROSS SECTION (CM**2)'
      READ*,AC
      R=SQRT(AC/PI)
      WRITE(*,*)'ENTER THRESHOLD LET (MEV-CM**2/MG)'
      READ*,LTH
      WRITE(*,*)'ENTER THICKNESS (CM)'
      READ*,T
      OPEN(UNIT=8,STATUS='OLD',FILE='HFLUX00.DAT')
      REWIND(8)
      READ(8,*)N
      READ(8,*)M
      A(1)=0.0
      A(N+1)=PI
      IF (N.GE.2) THEN
         DO 10 J=2,N
         READ(8,*) A(J)
         A(J)=A(J)*PI/180.0
10       CONTINUE
      END IF
```

```
      DO 20 J=1,M
      READ(8,*) L(J)
   20 CONTINUE
      CLOSE(8)
      DO 40 J=1,N
      JC1=MOD(J,10)
      JC2=(J-JC1)/10
      FLNM1=CHAR(JC2+48)//CHAR(JC1+48)
      FLNM2='HFLUX'//FLNM1//'.DAT'
      OPEN(UNIT=8,STATUS='OLD',FILE=FLNM2)
      REWIND(8)
      DO 30 K=1,M
      READ(8,*) HA(J,K)
      HA(J,K)=8.64*HA(J,K)
   30 CONTINUE
      CLOSE(8)
   40 CONTINUE
C Construct the B's using (13), the C's using (16),
C and the D's using (22).
      B(1)=0.0
      B(2)=ATAN(2.0*R/T)
      B(3)=PI2
      B(4)=PI-ATAN(2.0*R/T)
      B(5)=PI
      DO 60 I=1,4
      DO 50 J=1,N
      C1(I,J)=AMAX1(A(J),B(I))
      C2(I,J)=AMIN1(A(J+1),B(I+1))
   50 CONTINUE
   60 CONTINUE
      DO 70 J=1,N
      D1(1,J)=COS(C1(1,J))
      D1(2,J)=COS(C1(2,J))
      D1(3,J)=COS(PI-C1(3,J))
      D1(4,J)=COS(PI-C1(4,J))
      D2(1,J)=COS(C2(1,J))
      D2(2,J)=COS(C2(2,J))
      D2(3,J)=COS(PI-C2(3,J))
      D2(4,J)=COS(PI-C2(4,J))
   70 CONTINUE
C Construct S(K) using (32) and the F's using (33). The W's
C hold intermediate results and are reused in different
C calculations.
      DO 80 K=1,M
      W=2.0*R*L(K)/(T*LTH)
      W=1.0-W*W
      S(K)=0.0
      IF (W.GT.0.0) S(K)=SQRT(W)
      F3(K)=0.0
      IF (L(K).LE.LTH) THEN
         W=L(K)/LTH
         W1=2.0*R*R*W*W
         W2=R*T*W*SQRT(1.0-W*W)
         W3=R*T*ASIN(W)
         W4=(4.0/3.0)*R*T*(LTH/L(K))*(1.0-W*W)**1.5
```

```
            F3(K)=W1+W2+W3+W4
          END IF
          W=S(K)
          W1=2.0*R*R*W*W
          W2=R*T*W*SQRT(1.0-W*W)
          W3=R*T*ASIN(W)
          W4=(4.0/3.0)*R*T*(LTH/L(K))*(1.0-W*W)**1.5
          F4(K)=W1+W2+W3+W4
   80     CONTINUE
          DO 110 I=1,4
          DO 100 J=1,N
          DO 90 K=1,M
          W=D1(I,J)
          W1=2.0*R*R*W*W
          W2=R*T*W*SQRT(1.0-W*W)
          W3=R*T*ASIN(W)
          W4=(4.0/3.0)*R*T*(LTH/L(K))*(1.0-W*W)**1.5
          F1(I,J,K)=W1+W2+W3+W4
          W=D2(I,J)
          W1=2.0*R*R*W*W
          W2=R*T*W*SQRT(1.0-W*W)
          W3=R*T*ASIN(W)
          W4=(4.0/3.0)*R*T*(LTH/L(K))*(1.0-W*W)**1.5
          F2(I,J,K)=W1+W2+W3+W4
    90    CONTINUE
   100    CONTINUE
   110    CONTINUE
C  Now calculate G(J,K) using (31). The W's hold
C  intermediate results.
          DO 130 J=1,N
          DO 120 K=1,M
          W=L(K)/LTH
          U=S(K)
          W1=0.0
          IF ((C2(1,J).GT.C1(1,J)).AND.(W.GT.D2(1,J))) W1=F3(K)-F2(1,J,K)
          W2=0.0
          IF ((C2(1,J).GT.C1(1,J)).AND.(W.GT.D1(1,J))) W2=F1(1,J,K)-F3(K)
          W3=0.0
          IF ((C2(2,J).GT.C1(2,J)).AND.(D2(2,J).GT.U)) W3=F4(K)-F2(2,J,K)
          W4=0.0
          IF ((C2(2,J).GT.C1(2,J)).AND.(D1(2,J).GT.U)) W4=F1(2,J,K)-F4(K)
          W5=0.0
          IF ((C2(3,J).GT.C1(3,J)).AND.(D1(3,J).GT.U)) W5=F4(K)-F1(3,J,K)
          W6=0.0
          IF ((C2(3,J).GT.C1(3,J)).AND.(D2(3,J).GT.U)) W6=F2(3,J,K)-F4(K)
          W7=0.0
          IF ((C2(4,J).GT.C1(4,J)).AND.(W.GT.D1(4,J))) W7=F3(K)-F1(4,J,K)
          W8=0.0
          IF ((C2(4,J).GT.C1(4,J)).AND.(W.GT.D2(4,J))) W8=F2(4,J,K)-F3(K)
          G(J,K)=W1+W2+W3+W4+W5+W6+W7+W8
   120    CONTINUE
   130    CONTINUE
C  Calculate the sum in (29) and print the result.
          RATE=0.0
          DO 150 J=1,N
```

```
      DO 140 K=1,M-1
      RATE=RATE+(G(J,K+1)+G(J,K))*(HA(J,K)-HA(J,K+1))
140   CONTINUE
150   CONTINUE
      RATE=PI*RATE
      WRITE(*,*)'LTH =',LTH
      WRITE(*,*)'T =',T
      WRITE(*,*)'AC =',AC
      WRITE(*,*)'RATE =',RATE,' UPSETS/DAY'
      END
```

```
      PROGRAM EFFLUX
C Copyright (c) 1991, California Institute of Technology.
C U.S. Government Sponsorship under NASA Contract NAS7-918
C is acknowledged.
C
C This program is the same as NIFUR except that threshold
C LET (LTH), normal incident cross section (AC), and
C thickness (T) are not assigned by the user. AC is set
C equal to 1 cm**2 and LTH is assigned in a loop so that it
C is given each of the LET values that the flux is tabulated
C against. For each LTH, T is varied for a maximum upset rate.
C A tabulation of maximum rate versus LTH is the effective
C flux and is stored in the file EFFLUX.OUT.
      REAL LTH,L(200)
      CHARACTER*2,FLNM1
      CHARACTER*11,FLNM2
      DIMENSION A(31),B(5),C1(4,30),C2(4,30),D1(4,30),D2(4,30)
      DIMENSION S(200),RAT(200),TT(200),HA(30,200)
      DIMENSION F3(200),F4(200),F1(4,30,200),F2(4,30,200)
      DIMENSION G(30,200)
C Read data. The files HFLUX00.DAT, HFLUX01.DAT, ...,
C HFLUX09.DAT, HFLUX10.DAT, HFLUX11.DAT, ... contain
C environmental data. There is one file (after the "00" file)
C for each angular bin (discussed below). The angular inter-
C val [0,180 degrees) is partitioned into the bins
C [A(1),A(2)), [A(2),A(3)), ...,[A(N),A(N+1)) where A(1)=0
C and A(N+1)=180. The discrete values L(1), ...,L(M) of LET
C (in MeV-cm**2/mg) are selected by the user. The file
C HFLUX00.DAT contains the values of N, M, A(2), ..., A(N),
C L(1), ..., L(M) respectively. (Note that the A's are read
C in degrees and then converted into radians. Also note that,
C for an isotropic flux, N=1 and no A's are listed in
C HFLUX00.DAT.) The file HFLUX01.DAT contains the values of
C HA(1,1), HA(1,2), ..., HA(1,M) where HA(J,K) is the integral
C (in LET) directional flux ( in 1/m**2-sec-sr) evaluated at
C LET=L(K) and in the direction corresponding to the JTH
C angular bin. Etc. for the other files. Note that N must
C not exceed 30 and M must not exceed 200. After reading HA,
C convert to the units 1/cm**2-day-sr.
      PI=ATAN2(0.0,-1.0)
      PI2=ATAN2(1.0,0.0)
      AC=1.0
      R=SQRT(AC/PI)
      OPEN(UNIT=8,STATUS='OLD',FILE='HFLUX00.DAT')
      REWIND(8)
      READ(8,*)N
      READ(8,*)M
      A(1)=0.0
      A(N+1)=PI
      IF (N.GE.2) THEN
         DO 10 J=2,N
         READ(8,*) A(J)
         A(J)=A(J)*PI/180.0
```

```
 10      CONTINUE
       END IF
       DO 20 J=1,M
       READ(8,*) L(J)
 20    CONTINUE
       CLOSE(8)
       DO 40 J=1,N
       JC1=MOD(J,10)
       JC2=(J-JC1)/10
       FLNM1=CHAR(JC2+48)//CHAR(JC1+48)
       FLNM2='HFLUX'//FLNM1//'.DAT'
       OPEN(UNIT=8,STATUS='OLD',FILE=FLNM2)
       REWIND(8)
       DO 30 K=1,M
       READ(8,*) HA(J,K)
       HA(J,K)=8.64*HA(J,K)
 30    CONTINUE
       CLOSE(8)
 40    CONTINUE
C Start an outer loop in J1 that assigns values to LTH.
C An inner loop in J2 assigns values to T and calulates the
C upset rate. The maximum rate calculated in the inner loop
C is stored in RAT(J1) and the value of T producing this
C rate is stored in TT(J1).
       DO 210 J1=1,M
       LTH=L(J1)
       TT(J1)=0.0
       RAT(J1)=0.0
       DO 200 J2=1,21
       T=10.0**((FLOAT(J2)-21.0)/10.0)
C Now the upset rate calculation starts.
C Construct the B's using (13), the C's using (16),
C and the D's using (22).
       B(1)=0.0
       B(2)=ATAN(2.0*R/T)
       B(3)=PI2
       B(4)=PI-ATAN(2.0*R/T)
       B(5)=PI
       DO 60 I=1,4
       DO 50 J=1,N
       C1(I,J)=AMAX1(A(J),B(I))
       C2(I,J)=AMIN1(A(J+1),B(I+1))
 50    CONTINUE
 60    CONTINUE
       DO 70 J=1,N
       D1(1,J)=COS(C1(1,J))
       D1(2,J)=COS(C1(2,J))
       D1(3,J)=COS(PI-C1(3,J))
       D1(4,J)=COS(PI-C1(4,J))
       D2(1,J)=COS(C2(1,J))
       D2(2,J)=COS(C2(2,J))
       D2(3,J)=COS(PI-C2(3,J))
       D2(4,J)=COS(PI-C2(4,J))
 70    CONTINUE
C Construct S(K) using (32) and the F's using (33). The W's
```

```
C hold intermediate results and are reused in different
C calculations.
      DO 80 K=1,M
      W=2.0*R*L(K)/(T*LTH)
      W=1.0-W*W
      S(K)=0.0
      IF (W.GT.0.0) S(K)=SQRT(W)
      F3(K)=0.0
      IF (L(K).LE.LTH) THEN
         W=L(K)/LTH
         W1=2.0*R*R*W*W
         W2=R*T*W*SQRT(1.0-W*W)
         W3=R*T*ASIN(W)
         W4=(4.0/3.0)*R*T*(LTH/L(K))*(1.0-W*W)**1.5
         F3(K)=W1+W2+W3+W4
      END IF
      W=S(K)
      W1=2.0*R*R*W*W
      W2=R*T*W*SQRT(1.0-W*W)
      W3=R*T*ASIN(W)
      W4=(4.0/3.0)*R*T*(LTH/L(K))*(1.0-W*W)**1.5
      F4(K)=W1+W2+W3+W4
   80 CONTINUE
      DO 110 I=1,4
      DO 100 J=1,N
      DO 90 K=1,M
      W=D1(I,J)
      W1=2.0*R*R*W*W
      W2=R*T*W*SQRT(1.0-W*W)
      W3=R*T*ASIN(W)
      W4=(4.0/3.0)*R*T*(LTH/L(K))*(1.0-W*W)**1.5
      F1(I,J,K)=W1+W2+W3+W4
      W=D2(I,J)
      W1=2.0*R*R*W*W
      W2=R*T*W*SQRT(1.0-W*W)
      W3=R*T*ASIN(W)
      W4=(4.0/3.0)*R*T*(LTH/L(K))*(1.0-W*W)**1.5
      F2(I,J,K)=W1+W2+W3+W4
   90 CONTINUE
  100 CONTINUE
  110 CONTINUE
C Now calculate G(J,K) using (31). The W's hold
C intermediate results.
      DO 130 J=1,N
      DO 120 K=1,M
      W=L(K)/LTH
      U=S(K)
      W1=0.0
      IF ((C2(1,J).GT.C1(1,J)).AND.(W.GT.D2(1,J))) W1=F3(K)-F2(1,J,K)
      W2=0.0
      IF ((C2(1,J).GT.C1(1,J)).AND.(W.GT.D1(1,J))) W2=F1(1,J,K)-F3(K)
      W3=0.0
      IF ((C2(2,J).GT.C1(2,J)).AND.(D2(2,J).GT.U)) W3=F4(K)-F2(2,J,K)
      W4=0.0
      IF ((C2(2,J).GT.C1(2,J)).AND.(D1(2,J).GT.U)) W4=F1(2,J,K)-F4(K)
```

```
      W5=0.0
      IF ((C2(3,J).GT.C1(3,J)).AND.(D1(3,J).GT.U)) W5=F4(K)-F1(3,J,K)
      W6=0.0
      IF ((C2(3,J).GT.C1(3,J)).AND.(D2(3,J).GT.U)) W6=F2(3,J,K)-F4(K)
      W7=0.0
      IF ((C2(4,J).GT.C1(4,J)).AND.(W.GT.D1(4,J))) W7=F3(K)-F1(4,J,K)
      W8=0.0
      IF ((C2(4,J).GT.C1(4,J)).AND.(W.GT.D2(4,J))) W8=F2(4,J,K)-F3(K)
      G(J,K)=W1+W2+W3+W4+W5+W6+W7+W8
 120  CONTINUE
 130  CONTINUE
C Calculate the upset rate using (29).
      RATE=0.0
      DO 150 J=1,N
      DO 140 K=1,M-1
      RATE=RATE+(G(J,K+1)+G(J,K))*(HA(J,K)-HA(J,K+1))
 140  CONTINUE
 150  CONTINUE
      RATE=PI*RATE
C Store the maximum upset rate and associated value of T
C in RAT(J1) and TT(J1).
      IF (RATE.GT.RAT(J1)) THEN
         RAT(J1)=RATE
         TT(J1)=T
      END IF
 200  CONTINUE
 210  CONTINUE
C Record the data. The values of TT(J1) are of academic
C interest and can be obtained by inserting additional
C WRITE statements.
      OPEN(UNIT=8,STATUS='UNKNOWN',FILE='EFFLUX.OUT')
      REWIND(8)
      WRITE(8,*)'EFFECTIVE FLUX'
      WRITE(8,*)' '
      WRITE(8,*)'LET IN UNITS OF MeV-cm**2/mg'
      WRITE(8,*)'FLUX IN UNITS OF 1/(cm**2-day)'
      WRITE(8,*)' '
      WRITE(8,230)'LET','FLUX'
      WRITE(8,230)'---','----'
      DO 220 J=1,M
      WRITE(8,240) L(J),RAT(J)
 220  CONTINUE
      CLOSE(8)
 230  FORMAT(A28,A20)
 240  FORMAT(E31.4,E20.4)
      END
```

REFERENCES

[1] J.H. Adams, Jr., Cosmic Ray Effects on Microelectronics, Part IV, NRL Memorandum Report 5901, Dec.31,1986.

[2] L.D. Edmonds, "A Simple Estimate of Funneling-Assisted Charge Collection," IEEE Transactions on Nuclear Science, vol.38, no.2, pp. 828-833, April 1991.

[3] W.L. Bendel, Length Distribution of Chords Through a Rectangular Volume, NRL Memorandum Report 5369, July 3,1984.